arXiv:1605.02449v1 [cond-mat.str-el] 9 May 2016

New insights on frequency combinations and 'forbidden frequencies' in de Haas-van Alphen spectrum of κ-$(ET)_2Cu(SCN)_2$

Alain Audouard[1], Jean-Yves Fortin[2], David Vignolles[1],

Vladimir N. Laukhin[3,4], Nataliya D. Kushch[5] and Eduard B. Yagubskii[5]

[1] *Laboratoire National des Champs Magnétiques Intenses (UPR 3228 CNRS, INSA, UGA, UPS) 143 avenue de Rangueil, F-31400 Toulouse, France.*

[2] *Institut Jean Lamour, Département de Physique de la Matière et des Matériaux, CNRS-UMR 7198, Vandoeuvre-les-Nancy, F-54506, France*

[3] *Institució Catalana de Recerca i Estudis Avançats (ICREA), 08210 Barcelona, Spain.*

[4] *Institut de Ciència de Materials de Barcelona, Consejo Superior de Investigationes Científicas, Campus Universitat Autònoma de Barcelona, Bellaterra 08193, Spain.*

[5] *Institute of Problems of Chemical Physics, Russian Academy of Sciences, 142432 Chernogolovka, MD, Russia.*

(Dated: May 10, 2016)

Abstract

De Haas-van Alphen oscillations of the organic metal κ-$(ET)_2Cu(SCN)_2$ have been measured up to 55 T at liquid helium temperatures. The Fermi surface of this charge transfer salt is a textbook example of linear chain of orbits coupled by magnetic breakdown. Accordingly, the oscillation spectrum is composed of linear combinations of the frequencies linked to the α and magnetic breakdown-induced β orbits. The field and temperature dependence of all the observed Fourier components, in particular the 'forbidden frequency' $\beta - \alpha$ which cannot correspond to a classical orbit, are quantitatively accounted for by analytical calculations based on a second order development of the free energy, i.e. beyond the first order Lifshitz-Kosevich formula.

Keywords: Organic superconductors, high magnetic fields, quantum oscillations, Fermi surface

I. INTRODUCTION

The family of organic charge transfer salts κ-$(ET)_2X$, where ET stands for the bis(ethylenedithio)tetrathiafulvalene molecule and X is a monovalent cation, arouses interest for many years. Indeed, its members can be classified in a very rich phase diagram including ground states ranging from Mott insulator to superconductor [1, 2]. κ-$(ET)_2Cu(SCN)_2$, which has been synthesized as early as 1988 [3], is on the metallic side of this phase diagram and is still one of the most studied organic superconductor. Illustrating this long-standing interest, the existence of a Fulde-Ferrell-Larkin-Ovchinnikov inhomogeneous superconducting state in this salt, considered more than 20 years ago for low dimensional conductors [4, 5], have received first experimental hints in the early 2000s [6] and have been recently confirmed [7].

Remarkably, the Fermi surface of κ-$(ET)_2Cu(SCN)_2$ [8–10] (see Fig. 1) is the first experimental realization of the model Fermi surface proposed by Pippard in the early sixties to compute the effect of magnetic breakdown (MB) in multiband metals [11]. Both Shubnikov-de Haas (SdH) [12–19] and de Haas-van Alphen (dHvA) [20–24] oscillations have been widely studied in this compound. Provided the magnetic field strength is high enough to overcome the MB gap between the α orbit and the quasi one-dimensional sheets, linear combinations of the frequencies linked to the α and MB-induced β orbits are observed in the oscillatory spectrum (for a review see e.g. [26]), as expected in the framework of the coupled orbits network model of Falicov-Stachowiak [27]. Within this model, the frequency F_η of any Fourier component can be expressed as $F_\eta = n_\alpha F_\alpha + n_\beta F_\beta$ where $n_{\alpha(\beta)}$ is an integer and $F_{\alpha(\beta)}$ is the frequency linked to the $\alpha(\beta)$ orbit. With the exception of quantum interference (QI), which only holds for magnetoresistance, and for which the effective mass is the difference between the partial effective mass of each QI path [28], the effective mass m_η is given by $m_\eta = n_\alpha m_\alpha + n_\beta m_\beta$. However, limiting ourselves to dHvA data, the field and temperature dependence of few of the observed Fourier components does not behave consistently with this model. For example, the effective masses linked to 2α and 2β, determined in the framework of the Lifshitz-Kosevich model [29], are strongly different from $2m_\alpha$ and $2m_\beta$, respectively [22]. In addition, puzzling data are reported regarding the component $\beta + \alpha$ which corresponds to a MB orbit. Indeed, even though according to [21] $m_{\beta+\alpha}$ is equal to $m_\beta + m_\alpha$ within the error bars, in agreement with the Falicov-Stachowiak model, this relation

cannot account for the data of [22, 23] for which $m_{\beta+\alpha}$ is definitely smaller than the sum $m_\beta + m_\alpha$ (see [30] for a discussion of this feature). In addition to all this, the most striking discrepancy between the Falicov-Stachowiak model and the dHvA data (for which QI is not relevant since dHvA is only sensitive to the density of states) is the presence of the Fourier components $\beta - \alpha$ and $2(\beta - \alpha)$, known as 'forbidden frequencies' which cannot correspond to closed orbits (for a review, see [26, 31]).

These features have been addressed in the case of θ-phase salts belonging to the family θ-$(ET)_4MBr_4(C_6H_4Cl_2)$ for M = Co, Zn [30, 32, 33] which share with κ-$(ET)_2Cu(SCN)_2$ the same Fermi surface topology. Briefly, the strong two-dimensionality of these compounds is responsible for a significant oscillation of the chemical potential in magnetic field which requires a calculation of the free energy (canonical ensemble) up to the second-order in damping factors. In few cases, the first order term of the oscillatory magnetization, which corresponds to the usual Lifshitz-Kosevich formula [29], may have a smaller contribution to the amplitude of the Fourier components linked to MB orbits than the second order term. Moreover, the second order term solely accounts for the 'forbidden frequencies'. A very good quantitative agreement between these calculations and the reported dHvA data is observed. Nevertheless, as pointed out in [30], data analysis relevant to other salts, with different physical parameters, such as effective masses, MB field, *etc.*, are required. Therefore, the aim of this paper is to report on dHvA data of κ-$(ET)_2Cu(SCN)_2$ at high magnetic field. It is confirmed that the usual Lifshitz-Kosevich formalism cannot account for few of the Fourier component amplitudes such as 2α and, obviously, $\beta - \alpha$. In contrast, it is demonstrated that the above mentioned second order development holds for all the observed Fourier components.

II. EXPERIMENTAL

The studied crystal, with approximate dimensions $0.1 \times 0.1 \times 0.04$ mm^3, was synthesized by electrocrystallization technique. Magnetic torque measurements were performed in pulsed magnetic fields of up to 55 T with pulse decay duration of 0.36 s, in the temperature range from 1.7 K to 4.2 K. The angle between the magnetic field direction and the normal to the conducting plane was $\theta = 20°$. Fig. 1(a) displays magnetic torque data at 1.7 K. As expected, a strong hysteresis is observed in the superconducting state at low field due to

flow of magnetic flux either into or out of the crystal as the field either increases or decreases [34]. In contrast, data for up and down fields are indiscernible from each other in the range where oscillations are observed. This result indicates that any temperature change due to eventual eddy currents is negligible. In addition, torque interaction effect might have been considered since, due to magnetic torque, θ angle is liable to change during the field sweep for small cantilever stiffness and (or) high θ value [35]. In the present case, θ changes are always smaller than 0.1°, leading to negligibly small amplitude and frequency changes of at most 0.2 % at the highest fields explored. In the following, only data recorded during the decreasing part of the field is therefore considered. Analysis of the oscillatory part of the magnetic torque is based on discrete Fourier transforms of the data, after substraction of a smoothly varying background, calculated with a Blackman window.

III. RESULTS AND DISCUSSION

The high field range of the oscillatory part of the torque data is displayed in Fig. 1(a). As expected, corresponding Fourier analysis reveals several components, of which the frequencies are linear combinations of F_α and F_β. Owing to the tilt angle θ= 20°, these frequencies are $F_\alpha(\theta = 0) = 0.600(1)$ kT and $F_\beta(\theta = 0) = 3.861(7)$ kT. These values are in good agreement with the data of the literature [12–24] in which values in the range $F_\alpha(\theta = 0) =$ 0.596(2)-0.670(4) kT and $F_\beta(\theta = 0) =$ 3.8-3.923(9) kT are reported. The corresponding α orbit area amounts to 16 % of the first Brillouin zone area, in agreement with both previous experimental data and band structure calculations [8–10].

According to the calculations reported in Refs. [30, 32, 33], the amplitude of the basic α and β Fourier components, up to second order in damping factors, is accounted for by:

$$A_\alpha = -\frac{F_\alpha}{\pi m_\alpha} R_{\alpha,1} - \frac{F_\alpha}{\pi m_\beta}\left[\frac{1}{2}R_{\alpha,1}R_{\alpha,2} + \frac{1}{6}R_{\alpha,2}R_{\alpha,3} + 2R_{\beta,1}R_{\beta+\alpha,1} + \frac{1}{2}R_{\beta,2}R_{2\beta-\alpha,1}\right] \quad (1)$$

and

$$A_\beta = -\frac{F_\beta}{\pi m_\beta} R_{\beta,1} - \frac{F_\beta}{\pi m_\beta}\left[\frac{1}{2}R_{\beta,1}R_{\beta,2} + \frac{1}{6}R_{\beta,2}R_{\beta,3} + 2R_{\alpha,1}R_{\beta+\alpha,1} + 2R_{\beta,1}R_{2\beta,1}\right], \quad (2)$$

respectively. Damping factors can be expressed as $R_{\eta,p}(B,T) = R^T_{\eta,p}(B,T)R^D_{\eta,p}(B)R^{MB}_{\eta,p}(B)R^s_{\eta,p}$, where η stands either for α or β and p is the har-

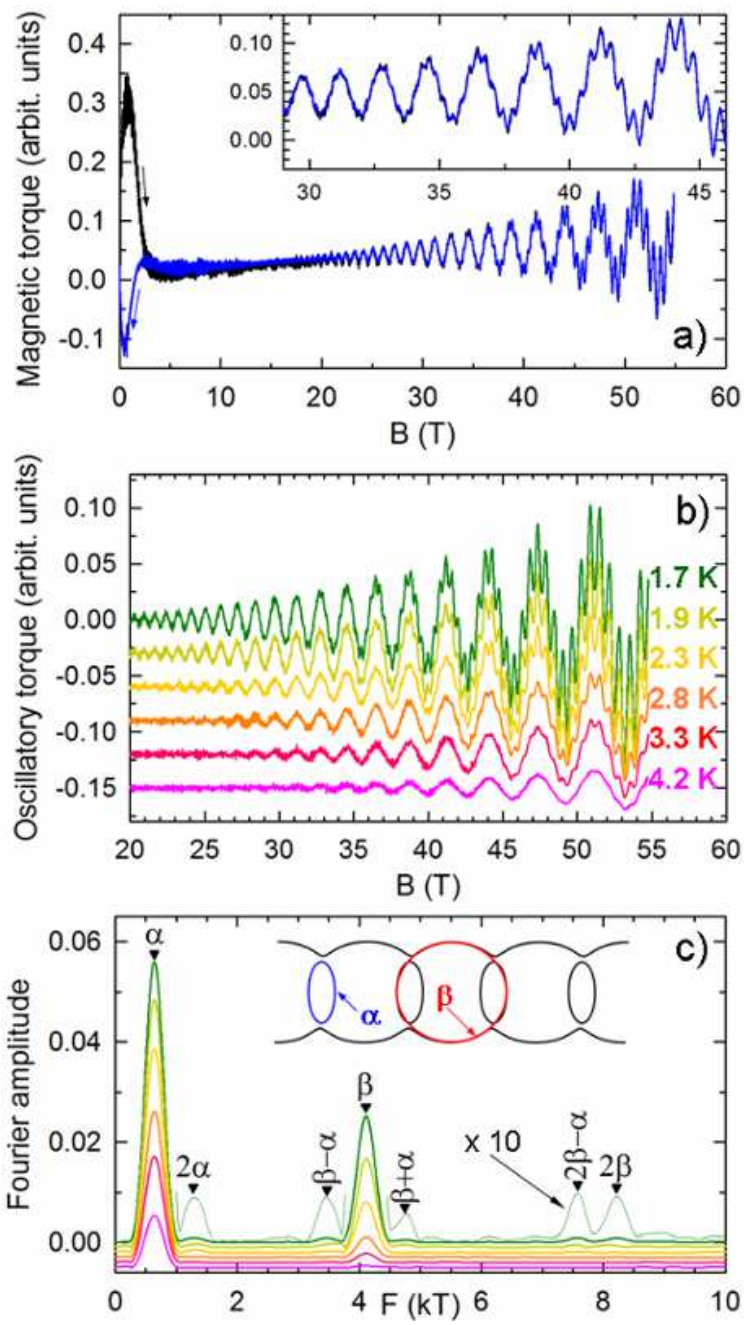

FIG. 1: (a) Field-dependent magnetic torque at T = 1.7 K. Black and blue lines stand for increasing and decreasing field sweeps, respectively. (b) Field-dependent oscillatory torque for decreasing field sweeps at various temperatures and (c) corresponding Fourier analysis in the field range 20-55 T. The angle between the magnetic field direction and the normal to the conducting plane is $\theta = 20°$. Marks are calculated with $F_\alpha(\theta = 0) = 0.600$ kT and $F_\beta(\theta = 0) = 3.861$ kT. The insert displays a sketch of the Fermi surface in which the α and β orbits are indicated.

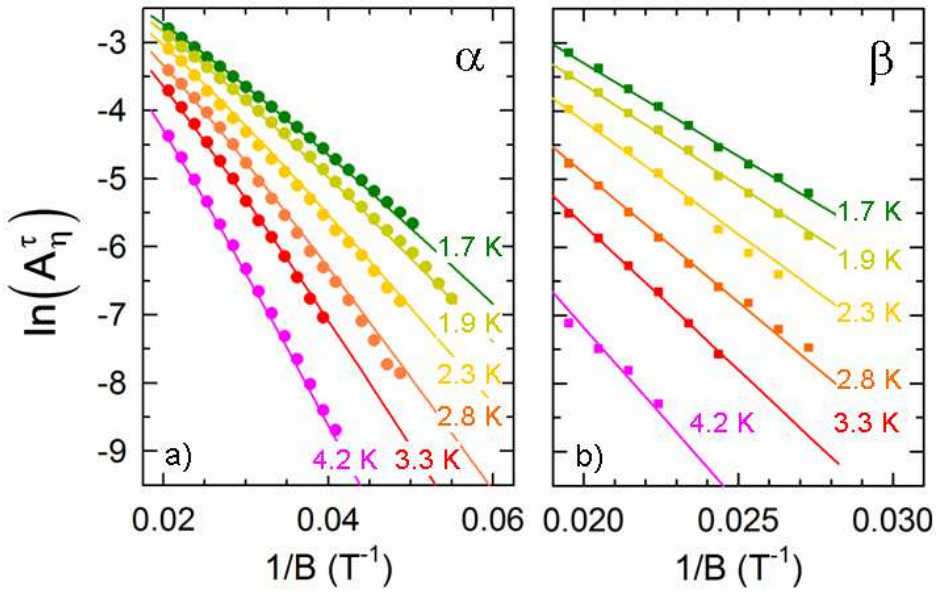

FIG. 2: Dingle plots of (a) α and (b) β Fourier components. Symbols are experimental Fourier amplitudes and solid lines in (a) and (b) are best fits of Eqs. 1 and 2 , respectively, obtained with $m_\alpha = 3.07$, $m_\beta = 6.03$, $T_D = 0.87$ K and $B_0 = 16$ T. Uncertainty on these parameters is given in the text.

monic number. For a two-dimensional Fermi surface, the thermal, Dingle, MB and spin damping factors are expressed as $R^T_{\eta,p} = pu_\eta \sinh^{-1}(pu_\eta)$, $R^D_{\eta,p} = \exp(-pu_0 m_\eta T_{D\eta}/B\cos\theta)$, $R^{MB}_{\eta,p} = (ip_0)^{n^t_\eta}(q_0)^{n^r_\eta}$ and $R^s_{\eta,p} = \cos(\pi g^*_\eta m_\eta/2\cos\theta)$, respectively [29]. The parameter (u_η) and the constant (u_0) are expressed as $u_\eta = u_0 m_\eta T/B\cos\theta$ and $u_0 = 2\pi^2 k_B m_e (e\hbar)^{-1} = 14.694$ T/K. $T_{D\eta}$ is the Dingle temperature defined by $T_D = \hbar(2\pi k_B \tau)^{-1}$, where τ^{-1} is the scattering rate. m_η and g_η are the effective mass (in m_e units) and effective Landé factor, respectively. The MB damping factor involves the number of tunnelings (n^t_η) and reflections (n^r_η) encountered by a quasiparticle traveling the orbit. The corresponding probabilities, p_0 and q_0=$(1-p_0^2)^{1/2}$, respectively, are given by the Chambers formula which involve the magnetic breakdown field B_0: $p_0^2 = e^{-B_0/B\cos\theta}$ [36].

The first order term of these equations just corresponds to the Lifshitz-Kosevich formula. Besides, provided that the spin damping factors $R^s_{\alpha(\beta)}$ are not too small (i.e. $m_\eta g_\eta/\cos\theta$) is not close to an odd integer), the second order term is negligible [30]. This point, which can be checked *a posteriori*, allows us to perform the data analysis relevant to α and β in the framework of Lifshitz-Kosevich formula. Nevertheless, even though the spin damping factors

act as constant prefactors in this case, 5 parameters are still involved, namely m_α, m_β, $T_{D\alpha}$, $T_{D\beta}$ and B_0. For this reason, it is assumed in the following that the Dingle temperature is the same for the α and β orbits ($T_{D\alpha}$=$T_{D\beta}$=T_D). Finally, it must be kept in mind that the magnetic torque amplitudes A_η^τ are related to the dHvA amplitude by $A_\eta^\tau = \tau_0 B A_\eta$ where τ_0 is a prefactor depending on the crystal mass, cantilever stiffness and tilt angle θ.

Dingle plots relevant to the α and β orbits are displayed in Fig. 2. A good agreement between the data and the calculations is obtained with m_α = 3.07(4), m_β = 6.03(11), T_D = 0.87(6) K and B_0 = 16(8) T. The effective mass values are within the range of the data reported in the literature in which m_α and m_β ranging from 3 to 3.6 and 5.6 to 7.1, respectively, can be found. In line with statement of Ref. [37], $m_\beta/m_\alpha = 2$ within the error bars.

It can be noticed that the MB field B_0 is obtained with a large uncertainty. This feature, can be explained considering that, in addition to an increase of the Dingle plot slope relevant to the β orbit, the main discernible effect of MB is to induce a curvature in the field dependence of the α amplitude. However, this curvature remains small in the explored field range which yields a large uncertainty. This uncertainty is reflected in the strong scattering of the previously reported experimental data which yield B_0 values (themselves with large uncertainties) in the range from 15 T to 45 T [17, 18, 21, 22, 24, 25].

Data relevant to frequency combinations are reported in Fig. 3. Let us consider first the component 2α, the amplitude of which is given by

$$A_{2\alpha} = -\frac{F_\alpha}{2\pi m_\alpha} R_{\alpha,2} + \frac{F_\alpha}{\pi m_\beta}\left[R_{\alpha,1}^2 - \frac{2}{3} R_{\alpha,1} R_{\alpha,3} - R_{\beta,2} R_{\beta+\alpha,2}\right]. \quad (3)$$

The first order term of Eq. 3, involving $R_{\alpha,2}$, corresponds to the Lifshitz formula. The second order term is dominated by the factor involving $R_{\alpha,1}^2$. Putting aside the spin damping factors, $R_{\alpha,1}^2$ is strictly equal to $R_{\alpha,2}$ as the ratio B/T goes to zero. In the explored high field range, $R_{\alpha,1}^2$ takes even larger values than $R_{\alpha,2}$. As a consequence, both the first and second order terms contribute to the amplitude. Hence, the two involved spin damping factors, $R_{\alpha,2}^s$ and $R_{\alpha,1}^s$, must be taken into account. Solid lines in Fig. 3(a) are best fits of Eq. 3. They are obtained with the same effective masses, Dingle temperature and magnetic breakdown field as for the data relevant to α and β (see Fig. 2) and with g_α = 1.73(5). This latter value is slightly larger than deduced from the angle dependence of the α oscillations (g_α = 1.63(8) [21]). Nevertheless, it can be remarked that the product $g_\alpha m_\alpha$ = 5.6(2), governing the spin

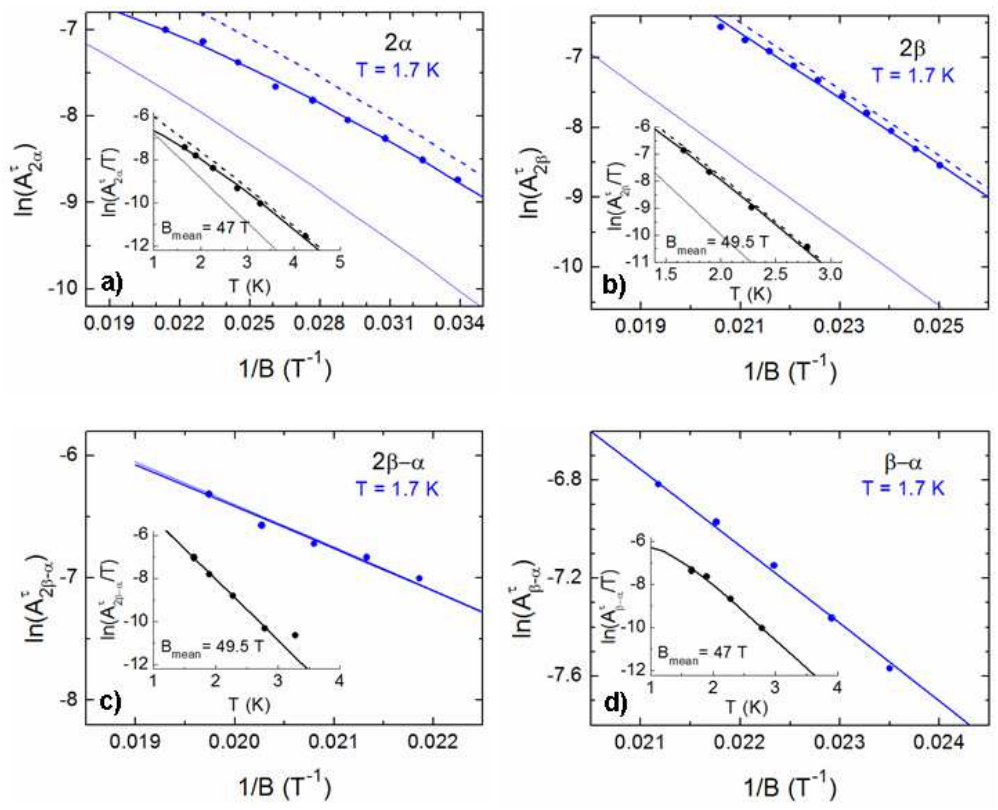

FIG. 3: Dingle plots of (a) 2α, (b) 2β, (c) $2\beta - \alpha$ and (d) $\beta - \alpha$ Fourier components. Mass plots are reported in the inserts. Symbols are experimental Fourier amplitudes and solid lines are best fits of Eqs. 3, 4, 5 and 6, respectively, to the data, obtained with the same parameters as in Fig. 2 and with $g^*_\alpha = 1.73$ and $g^*_\beta = 1.52$. Uncertainty on these parameters is given in the text. Thin solid and dashed lines are the contribution of the first (i.e. Lifshitz-Kosevich) and second order terms, respectively, of the above mentioned equations.

damping factor is close to the value, $g_\alpha m_\alpha = 5.2(5)$, obtained in Ref. [21]. Strikingly, it can be observed that the second order term has a dominant contribution to the amplitude of the component 2α.

Similar considerations hold for 2β. Indeed, its amplitude is accounted for by

$$A_{2\beta} = -\frac{F_\beta}{2\pi m_\beta}\left[R_{\beta,2} + 2R_{2\beta,1}\right] + \frac{F_\beta}{\pi m_\beta}\left[R^2_{\beta,1} - \frac{2}{3}R_{\beta,1}R_{\beta,3} - \frac{1}{4}R_{\beta,2}R_{\beta,4} - R_{\alpha,2}R_{\beta+\alpha,2}\right. \quad (4)$$
$$\left. + 2R_{\alpha,1}R_{2\beta-\alpha,1} - R_{\beta,2}R_{2\beta,2} - R_{\beta,4}R_{2\beta,1}\right].$$

The Lifshitz-Kosevich contribution arises from both the magnetic breakdown orbit 2β involving 4 tunneling and 2 reflections and the second harmonics of β governed by $R_{2\beta,1}$

and $R_{\beta,2}$, respectively (see [30] for a discussion of this point). The factors $R^2_{\beta,1}$, and to a less extent $R_{\alpha,1}R_{2\beta-\alpha,1}$, appearing in Eq. 4 play a role similar to $R^2_{\alpha,1}$ in Eq. 3, the other second order factors being negligible. Solid lines in Fig. 3(b) are best fits of Eq. 4. They are obtained with the same set of parameters as in Fig. 2 and $g_\beta = 1.52(12)$ which is just the value given in Ref. [24]. Similarly to 2α, the second order term dominates the amplitude of 2β.

The amplitude of the component $2\beta - \alpha$, which corresponds to a classical magnetic breakdown orbit involving 4 tunneling and 2 reflections, is given by

$$A_{2\beta-\alpha} = -\frac{F_{2\beta-\alpha}}{\pi m_{2\beta-\alpha}} R_{2\beta-\alpha,1} - \frac{F_{2\beta-\alpha}}{\pi m_\beta}\left[\frac{1}{2}R_{\alpha,1}R_{\beta,2} + \frac{1}{3}R_{\alpha,3}R_{\beta+\alpha,2}\right]. \tag{5}$$

The second order term is dominated by the product $R_{\alpha,1}R_{\beta,2}$ which is much lower than the damping factor $R_{2\beta-\alpha,1}$ entering the Lifshitz-Kosevich formula, provided the spin damping factor $R^s_{2\beta-\alpha}$ is not too small. For this reason, the Lifshitz-Kosevich formula holds for this orbit as it is the case for the above considered α and β orbits and accounts for the data of Fig. 3(c).

Finally, the 'forbidden orbit' $\beta - \alpha$ is accounted for by

$$A_{\beta-\alpha} = -\frac{F_{\beta-\alpha}}{\pi m_\beta}\left[R_{\alpha,1}R_{\beta,1} + R_{\alpha,2}R_{\beta+\alpha,1} + R_{\beta,2}R_{\beta+\alpha,1} + R_{\beta,1}R_{2\beta-\alpha,1}\right]. \tag{6}$$

Since this component does not correspond to a classical orbit, only a second order term, dominated by the product $R_{\alpha,1}R_{\beta,1}$, enters the amplitude. Solid line in Fig. 3(d) are best fits to Eq. 6. They are obtained with the same set of parameters as in Fig. 2, as well. A very good agreement is observed.

IV. SUMMARY AND CONCLUSION

De Haas-van Alphen oscillations of the quasi-two dimensional organic metal κ-$(ET)_2Cu(SCN)_2$ have been studied at high magnetic field. The Fermi surface of this emblematic organic metal is a prime example of a linear chain of orbits coupled by magnetic breakdown. Accordingly, the oscillation spectrum is composed of linear combinations of the frequencies linked to the α and magnetic breakdown-induced β orbits. The field and temperature dependence of the observed Fourier components is consistently analyzed in the framework of analytical calculations based on a second order development of the free

energy taking into account the oscillations of the chemical potential, i.e. beyond the first order Lifshitz-Kosevich formula, and with the same set of parameters [m_α = 3.07(4), m_β = 6.03(11), T_D = 0.87(6) K, B_0 = 16(8) T, g_α = 1.73(5) and g_β = 1.52(12)] for all the considered components. A very good quantitative agreement with the experimental data is observed. Even though the data relevant to the classical orbits α, β and 2β-α follow the Lifshitz-Kosevich formula due to negligible second order terms, these second order terms strongly enters the field- and temperature-dependent amplitude of the components 2α, 2β and alone are responsible for the 'forbidden frequency' β-α.

Acknowledgments

The support of the European Magnetic Field Laboratory (EMFL) is acknowledged. The work was partially supported by the RFBR grant 14-03-00119-a and Program N2 of the Presidium of Russian Academy of Science.

[1] Kanoda K, J. Phys. Soc. Jpn., **75** 051007 (2006).

[2] Ardavan A, Brown S, Kagoshima S,Kanoda K , Kuroki K, Mori H,Ogata M , Uji S and Wosnitza J, J. Phys. Soc. Japan **81** 011004 (2012).

[3] Urayama H, Yamochi H, Saito G, Nozawa K, Sugano T, Kinoshita M, Sato S, Oshima K, Kawamoto A and Tanaka J, Chem. Lett. **1** 55 (1988).

[4] Shimahara H, Phys. Rev. B **50** 12760 (1994).

[5] Dupuis N, Phys. Rev. B **51**, 9074 (1995).

[6] Singleton J, J. Phys.: Condens. Matter **12** L641 (2000).

[7] Mayaffre H, Krämer S, Horvatic M, Berthier C, Miyagawa K, Kanoda K and Mitrovic V F, Nature Physics **10** 928 (2014).

[8] Oshima K, Mori T, Inokuchi H, Urayama H, Yamochi H and Saito G, Phys. Rev. B **38** 938 (1988).

[9] Jung D, Evain M, Novoa J J, Whangbo M-H, Beno M A, Kini A M, Schultz A J, Williams J M, and Nigrey P J, Inorg. Chem. **28** 4516 (1989).

[10] Campos C E, Sandhu P S, Brooks J S and Ziman T, Phys. Rev. B **53** 12725 (1996).

[11] Pippard A B, Proc. Roy. Soc. (London) **A270** 1 (1962).

[12] Toyota N, Sasaki T, Murata K, Honda Y, Tokumoto M, Bando H, Kinoshita N, Anzai H, Ishiguro T and Muto Y, J. Phys. Soc. Jpn. **57** 2616 (1988).

[13] Müller H, Heidmann C-P, Lerf A, Biberacher W, Sieburger R and Andres K, Springer Proceedings in Physics, Vol. 51, The Physics and Chemistry of Organic Superconductors, eds. G. Saito and S. Kagoshima, p. 195, Springer-Verlag Berlin, Heidelberg 1990.

[14] Sasaki T, Sato H and Toyota N, Solid State Commun. **76** 507 (1990).

[15] Andres K, Heidmann C-P, Müller H, Himmelsbach S, Biberacher W, Probst Ch and Joss W, Synth. Met. **42** 1893 (1991).

[16] Heidmann C-P, Müller H, Biberacher W, Neumaier K, Probst Ch and Andres K, Synth. Met. **42** 2029 (1991).

[17] Caulfield J, Lubczynski W, Pratt F L, Singleton J, Ko D Y K, Hayes W, Kurmoo M and Day P, J. Phys.: Condens. Matter **6** (1994) 2911.

[18] Harrison N, Caulfield J, Singleton J, Reinders P H P, Herlach F, Hayes W, Kurmoo M and Day P, J. Phys.-Condens. Matter **8** 5415 (1996).

[19] Kartsovnik M V, Logvenov G Yu, Ishiguro T, Biberacher W, Anzai H, Kushch N D, Phys. Rev. Lett. **77** 2530 (1996).

[20] Wosnitza J, Crabtree G W, Wang H H, Geiser U, Williams J M and Carlson K D, Phys. Rev. B **45** 3018 (1992).

[21] Meyer F A, Steep E, Biberacher W, Christ P, Lerf A, Jansen A G M, Joss W, Wyder P and Andres K, EPL **32** 681 (1995).

[22] Uji S, Chaparala M, Hill S, Sandhu P S, Qualls J, Seger L and Brooks J S, Synth. Met. **85** 1573 (1997).

[23] Steep E, Nguyen L H, Biberacher W, Müller H, Jansen A G M, Wyder P, Physica B **259-261** 1079 (1999).

[24] Gvozdikov V M, Pershin Y V, Steep E, Jansen A G M, and Wyder P, Phys. Rev. B **65** 165102 (2002).

[25] I. Mihut, C. C. Agosta, C. Martin, C. H. Mielke, T. Coffey, M. Tokumoto, M. Kurmoo, J. A. Schlueter, P. Goddard and N. Harrison, Phys. Rev. B **73** 125118 (2006).

[26] Uji S and Brooks J S, The Physics of Organic Superconductors and Conductors, Springer Series Material Science Vol. 110 (Springer, 2008), p. 89.

[27] Falicov L M and Stachowiak H, Phys. Rev. **147** 505 (1966).

[28] Stark R W and Friedberg C B, Phys. Rev. Lett. **26** 556 (1971).

[29] Shoenberg D, Magnetic Oscillations in Metals (Cambridge University Press, Cambridge, 1984).

[30] Audouard A and Fortin J-Y, Low Temp. Phys. **40** 344 (2014), [Fiz. Nizk. Temp. **40** 444 (2014)].

[31] Kartsovnik M, Chem. Rev. **104** 5737 (2004).

[32] Audouard A, Fortin J-Y, Vignolles D, Lyubovskii R B, Drigo L, Duc F, Shilov G V, Ballon G, Zhilyaeva E I, Lyubovskaya R N and Canadell E, EPL **97** 57003 (2012).

[33] Audouard A, Fortin J-Y, Vignolles D, Lyubovskii R B, Drigo L, Shilov G V, Duc F, Zhilyaeva E I, Lyubovskaya R N and Canadell E, J. Phys.: Condens. Matter **27** 315601 (2015).

[34] Mola M M, Hill S, Brooks J S and Qualls J S, Phys. Rev. Lett. **86** 2130 (2001).

[35] Bergemann C, Julian SR, Mackenzie A P, Tyler A W, Farrell D E, Maeno Y and NishiZaki S, Physica C **317-318** 444 (1999).

[36] Chambers R G, Magnetic breakdown in real metals, Proc. Phys. Soc. **88** 701 (1966).

[37] Merino J and McKenzie R H, Phys. Rev. B **62** 2416 (2000).